
Multi-objective Bayesian optimisation with preferences over objectives

Majid Abdolshah, Alistair Shilton, Santu Rana, Sunil Gupta, Svetha Venkatesh

The Applied Artificial Intelligence Institute (A²I²),

Deakin University, Australia

{majid, alistair.shilton, santu.rana, sunil.gupta, svetha.venkatesh}
@deakin.edu.au

Abstract

We present a multi-objective Bayesian optimisation algorithm that allows the user to express preference-order constraints on the objectives of the type “objective A is more important than objective B”. These preferences are defined based on the stability of the obtained solutions with respect to preferred objective functions. Rather than attempting to find a representative subset of the complete Pareto front, our algorithm selects those Pareto-optimal points that satisfy these constraints. We formulate a new acquisition function based on expected improvement in dominated hypervolume (EHI) to ensure that the subset of Pareto front satisfying the constraints is thoroughly explored. The hypervolume calculation is weighted by the probability of a point satisfying the constraints from a gradient Gaussian Process model. We demonstrate our algorithm on both synthetic and real-world problems.

1 Introduction

In many real world problems, practitioners are required to sequentially evaluate a noisy black-box and expensive to evaluate function f with the goal of finding its optimum in some domain \mathbb{X} . Bayesian optimisation is a well-known algorithm for such problems. There are variety of studies such as hyperparameter tuning [28, 14, 13], expensive multi-objective optimisation for Robotics [2, 1], and experimentation optimisation in product design such as short polymer fiber materials [17].

Multi-objective Bayesian optimisation involves at least two conflicting, black-box, and expensive to evaluate objectives to be optimised simultaneously. Multi-objective optimisation usually assumes that all objectives are *equally important*, and solutions are found by seeking the Pareto front in the objective space [4, 5, 3]. However, in most cases, users can stipulate preferences over objectives. This information will impart on the relative importance on sections of the Pareto front. Thus using this information to preferentially sample the Pareto front will boost the efficiency of the optimiser, which is particularly advantageous when the objective functions are expensive.

In this study, preferences over objectives are stipulated based on the stability of the solutions with respect to a set of objective functions. As an example, there are scenarios when investment strategists are looking for Pareto optimal investment strategies that prefer stable solutions for return (objective 1) but more diverse solutions with respect to risk (objective 2) as they can later decide their appetite for risk. As can be inferred, the stability in one objective produces more diverse solutions for the other objectives. We believe in many real-world problems our proposed method can be useful in order to reduce the cost, and improve the safety of experimental design.

Whilst multi-objective Bayesian optimisation for sample efficient discovery of Pareto front is an established research track [10, 19, 9, 16], limited work has examined the incorporation of preferences. Recently, there has been a study [19] wherein given a user specified preferred region in objective space,

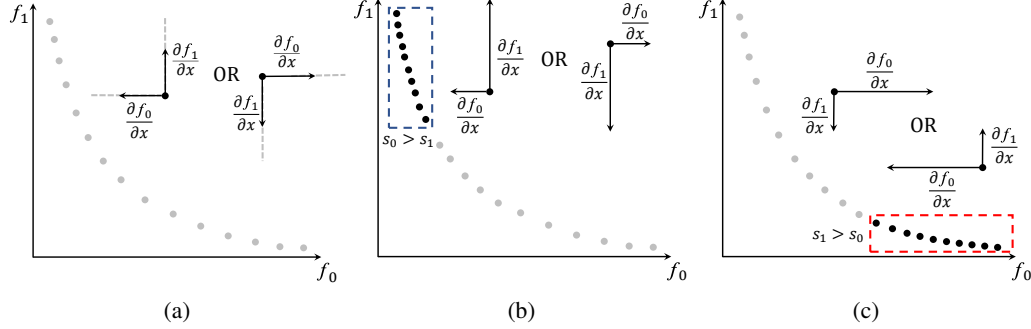


Figure 1: (a) Local Pareto optimality for 2 objective example with 1D design space. Local optimality implies $\frac{\partial f_0(x)}{\partial x}$ and $\frac{\partial f_1(x)}{\partial x}$ have opposite signs since the weighted sum of gradients of the objectives with respect to x must be zero: $\mathbf{s}^T \frac{\partial}{\partial x} \mathbf{f}(x) = 0$. In (b) we additionally require that $\|\frac{\partial f_1(x)}{\partial x}\| > \|\frac{\partial f_0(x)}{\partial x}\|$, so perturbation of x will cause relatively more change in f_1 than f_0 - i.e. such solutions are (relatively) stable in objective f_0 . (c) Shows the converse, namely $\|\frac{\partial f_0(x)}{\partial x}\| > \|\frac{\partial f_1(x)}{\partial x}\|$ favoring solutions that are (relatively) stable in objective f_1 and diverse in f_0 .

the optimiser focuses its sampling to derive the Pareto front efficiently. However, such preferences are based on the assumption of having an accurate prior knowledge about objective space and the preferred region (generally a hyperbox) for Pareto front solutions. The main contribution of this study is formulating the concept of preference-order constraints and incorporating that into a multi-objective Bayesian optimisation framework to address the unavailability of prior knowledge and boosting the performance of optimisation in such scenarios.

We are formulating the preference-order constraints through ordering of derivatives and incorporating that into multi-objective optimisation using the geometry of the constraints space whilst needing no prior information about the functions. Formally, we find a representative set of Pareto-optimal solutions to the following multi-objective optimisation problem:

$$\mathbb{D}^* \subset \mathbb{X}^* = \underset{\mathbf{x} \in \mathbb{X}}{\operatorname{argmax}} \mathbf{f}(\mathbf{x}) \quad (1)$$

subject to *preference-order constraints* - that is, assuming $\mathbf{f} = [f_0, f_1, \dots, f_m]$, f_0 is more important (in terms of stability) than f_1 and so on. Our algorithm aims to maximise the dominated hypervolume of the solution in a way that the solutions that meet the constraints are given more *weights*.

To formalise the concept of preference-order constraints, we first note that a point is locally Pareto optimal if any sufficiently small perturbation of a single design parameter of that point does not simultaneously increase (or decrease) all objectives. Thus, equivalently, a point is locally Pareto optimal if we can define a set of weight vectors such that, for each design parameter, the weighted sum of gradients of the objectives with respect to that design parameter is zero (see Figure 1a). Therefore, the weight vectors define the relative importance of each objective at that point. Figure 1b illustrates this concept where the blue box defines the region of stability for the function f_0 . Since in this section the magnitude of partial derivative for f_0 is smaller compared to that of f_1 , the weights required to satisfy Pareto optimality would need higher weight corresponding to the gradient of f_0 compared to that of f_1 (see Figure 1b). Conversely, in Figure 1c, the red box highlights the section of the Pareto front where solutions have high stability in f_1 . To obtain samples from this section of the Pareto front, we need to make the weights corresponding to the gradient of f_0 to be smaller to that of the f_1 .

Our solution is based on understanding the geometry of the constraints in the weight space. We show that preference order constraints gives rise to a polyhedral proper cone in this space. We show that for the pareto-optimality condition, it necessitates the gradients of the objectives at pareto-optimal points to lie in a perpendicular cone to that polyhedral. We then quantify the posterior probability that any point satisfies the preference-order constraints given a set of observations. We show how these posterior probabilities may be incorporated into the EHI acquisition function [12] to steer the Bayesian optimiser toward Pareto optimal points that satisfy the preference-order constraint and away from those that do not.

2 Notation

Sets are written $\mathbb{A}, \mathbb{B}, \mathbb{C}, \dots$ where \mathbb{R}_+ is the positive reals, $\bar{\mathbb{R}}_+ = \mathbb{R}_+ \cup \{0\}$, $\mathbb{Z}_+ = \{1, 2, \dots\}$, and $\mathbb{Z}_n = \{0, 1, \dots, n-1\}$. $|\mathbb{A}|$ is the cardinality of the set \mathbb{A} . Tuples (ordered sets) are denoted $\mathfrak{A}, \mathfrak{B}, \mathfrak{C}, \dots$. Distributions are denoted $\mathcal{A}, \mathcal{B}, \mathcal{C}, \dots$. Column vectors are bold lower case $\mathbf{a}, \mathbf{b}, \mathbf{c}, \dots$. Matrices bold upper case $\mathbf{A}, \mathbf{B}, \mathbf{C}, \dots$. Element i of vector \mathbf{a} is a_i , and element i, j of matrix \mathbf{A} is $A_{i,j}$ (all indexed $i, j = 0, 1, \dots$). The transpose is denoted $\mathbf{a}^\top, \mathbf{A}^\top$. \mathbf{I} is the identity matrix, $\mathbf{1}$ is a vector of 1s, $\mathbf{0}$ is a vector of 0s, and \mathbf{e}_i is a vector $e_{(i)j} = \delta_{ij}$, where δ_{ij} is the Kronecker-Delta. $\nabla_{\mathbf{x}} = [\frac{\partial}{\partial x_0} \quad \frac{\partial}{\partial x_1} \quad \dots \quad \frac{\partial}{\partial x_{n-1}}]^\top$, $\text{sgn}(x)$ is the sign of x (where $\text{sgn}(0) = 0$), and the indicator function is denoted as $\mathbb{1}(\mathbb{A})$.

3 Background

3.1 Gaussian Processes

Let $\mathbb{X} \subset \mathbb{R}^n$ be compact. A Gaussian process [24] $\mathcal{GP}(\mu, K)$ is a distribution on the function space $f : \mathbb{X} \rightarrow \mathbb{R}$ defined by mean $\mu : \mathbb{X} \rightarrow \mathbb{R}$ (assumed zero without loss of generality) and kernel (covariance) $K : \mathbb{X} \times \mathbb{X} \rightarrow \mathbb{R}$. If $f(\mathbf{x}) \sim \mathcal{GP}(0, K(\mathbf{x}, \mathbf{x}'))$ then the posterior of f given $\mathbb{D} = \{(\mathbf{x}_{(j)}, y_{(j)}) \in \mathbb{R}^n \times \mathbb{R} | y_{(j)} = f(\mathbf{x}_{(j)}) + \epsilon, \epsilon \sim \mathcal{N}(0, \sigma^2), j \in \mathbb{Z}_N\}$, $f(\mathbf{x}) | \mathbb{D} \sim \mathcal{N}(\mu_{\mathbb{D}}(\mathbf{x}), \sigma_{\mathbb{D}}(\mathbf{x}, \mathbf{x}'))$, where:

$$\begin{aligned} \mu_{\mathbb{D}}(\mathbf{x}) &= \mathbf{k}^\top(\mathbf{x}) (\mathbf{K} + \sigma^2 \mathbf{I})^{-1} \mathbf{y} \\ \sigma_{\mathbb{D}}(\mathbf{x}, \mathbf{x}') &= K(\mathbf{x}, \mathbf{x}') - \mathbf{k}^\top(\mathbf{x}) (\mathbf{K} + \sigma^2 \mathbf{I})^{-1} \mathbf{k}(\mathbf{x}') \end{aligned} \quad (2)$$

and $\mathbf{y}, \mathbf{k}(\mathbf{x}) \in \mathbb{R}^{|\mathbb{D}|}$, $\mathbf{K} \in \mathbb{R}^{|\mathbb{D}| \times |\mathbb{D}|}$, $k(\mathbf{x})_j = K(\mathbf{x}, \mathbf{x}_{(j)})$, $K_{jk} = K(\mathbf{x}_{(j)}, \mathbf{x}_{(k)})$.

Since differentiation is a linear operation, the derivative of a Gaussian process is also a Gaussian process [18, 23]. The posterior of $\nabla_{\mathbf{x}} f$ given \mathbb{D} is $\nabla_{\mathbf{x}} f(\mathbf{x}) | \mathbb{D} \sim \mathcal{N}(\boldsymbol{\mu}'_{\mathbb{D}}(\mathbf{x}), \boldsymbol{\sigma}'_{\mathbb{D}}(\mathbf{x}, \mathbf{x}'))$, where:

$$\begin{aligned} \boldsymbol{\mu}'_{\mathbb{D}}(\mathbf{x}) &= (\nabla_{\mathbf{x}} \mathbf{k}^\top(\mathbf{x})) (\mathbf{K} + \sigma^2 \mathbf{I})^{-1} \mathbf{y} \\ \boldsymbol{\sigma}'_{\mathbb{D}}(\mathbf{x}, \mathbf{x}') &= \nabla_{\mathbf{x}} \nabla_{\mathbf{x}'}^\top K(\mathbf{x}, \mathbf{x}') - (\nabla_{\mathbf{x}} \mathbf{k}^\top(\mathbf{x})) (\mathbf{K} + \sigma^2 \mathbf{I})^{-1} (\nabla_{\mathbf{x}'} \mathbf{k}^\top(\mathbf{x}'))^\top \end{aligned} \quad (3)$$

3.2 Multi-Objective Optimisation

A multi-objective optimisation problem has the form:

$$\underset{\mathbf{x} \in \mathbb{X}}{\text{argmax}} \mathbf{f}(\mathbf{x}) \quad (4)$$

where the components of $\mathbf{f} : \mathbb{X} \subset \mathbb{R}^n \rightarrow \mathbb{Y} \subset \mathbb{R}^m$ represent the m distinct objectives $f_i : \mathbb{X} \rightarrow \mathbb{R}$. \mathbb{X} and \mathbb{Y} are called design space and objective space, respectively. A Pareto-optimal solution is a point $\mathbf{x}^* \in \mathbb{X}$ for which it is not possible to find another solution $\mathbf{x} \in \mathbb{X}$ such that $f_i(\mathbf{x}) > f_i(\mathbf{x}^*)$ for all objectives f_0, f_1, \dots, f_{m-1} . The set of all Pareto optimal solutions is the Pareto set $\mathbb{X}^* = \{\mathbf{x}^* \in \mathbb{X} | \nexists \mathbf{x} \in \mathbb{X} : \mathbf{f}(\mathbf{x}) \succ \mathbf{f}(\mathbf{x}^*)\}$ where $\mathbf{y} \succ \mathbf{y}'$ (\mathbf{y} dominates \mathbf{y}') means $\mathbf{y} \neq \mathbf{y}'$, $y_i \geq y'_i \forall i$, and $\mathbf{y} \succeq \mathbf{y}'$ means $\mathbf{y} \succ \mathbf{y}'$ or $\mathbf{y} = \mathbf{y}'$.

Given observations $\mathbb{D} = \{(\mathbf{x}_{(j)}, \mathbf{y}_{(j)}) \in \mathbb{R}^n \times \mathbb{R}^m | \mathbf{y}_{(j)} = \mathbf{f}(\mathbf{x}_{(j)}) + \boldsymbol{\epsilon}, \epsilon_i \sim \mathcal{N}(0, \sigma_i^2)\}$ of \mathbf{f} the dominant set $\mathbb{D}^* = \{(\mathbf{x}^*, \mathbf{y}^*) \in \mathbb{D} | \nexists (\mathbf{x}, \mathbf{y}) \in \mathbb{D} : \mathbf{y} \succeq \mathbf{y}^*\}$ is the most optimal subset of \mathbb{D} (in the Pareto sense). The ‘‘goodness’’ of \mathbb{D} is often measured by the dominated hypervolume (S -metric, [32, 11]) with respect to some reference point $\mathbf{z} \in \mathbb{R}^m$: $S(\mathbb{D}) = S(\mathbb{D}^*) = \int_{\mathbf{y} \succeq \mathbf{z}} \mathbf{1}(\exists \mathbf{y}_{(i)} \in \mathbb{D} | \mathbf{y}_{(i)} \succeq \mathbf{y}) d\mathbf{y}$. Thus our aim is to find the set \mathbb{D} that maximises the hypervolume. Optimised algorithms exist for calculating hypervolume [30, 26], $S(\mathbb{D})$, which is typically calculated by sorting the dominant observations along each axis in objective space to form a grid. Dominated hypervolume (with respect to \mathbf{z}) is then the sum of the hypervolumes of the dominated cells (c_k) - i.e. $S(\mathbb{D}) = \sum_k \text{vol}(c_k)$.

3.3 Bayesian Multi-Objective Optimisation

In the multi-objective case one typically assumes that the components of \mathbf{f} are draws from independent Gaussian processes, i.e. $f_i(\mathbf{x}) \sim \mathcal{GP}(0, K_{(i)}(\mathbf{x}, \mathbf{x}'))$, and f_i and $f_{i'}$ are independent $\forall i \neq i'$. A

popular acquisition function for multi-objective Bayesian optimisation is expected hypervolume improvement (EHI). The EHI acquisition function is defined by:

$$a_t(\mathbf{x} | \mathbb{D}) = \mathbb{E}_{\mathbf{f}(\mathbf{x}) | \mathbb{D}} [\mathcal{S}(\mathbb{D} \cup \{(\mathbf{x}, \mathbf{f}(\mathbf{x}))\}) - \mathcal{S}(\mathbb{D})] \quad (5)$$

[27, 31] and represents the expected change in the dominated hypervolume by the set of observations based on the posterior Gaussian process.

4 Problem Formulation

Let $\mathbf{f} : \mathbb{X} \subset \mathbb{R}^n \rightarrow \mathbb{Y} \subset \mathbb{R}^m$ be a vector of m independent draws $f_i \sim \mathcal{GP}(0, K_{(i)}(\mathbf{x}, \mathbf{x}))$ from zero-mean Gaussian processes. Assume that \mathbf{f} is expensive to evaluate. Our aim is to find a representative set of Pareto-optimal solutions to the following multi-objective optimisation problem:

$$\mathbb{D}^* \subset \mathbb{X}^* = \operatorname{argmax}_{\mathbf{x} \in \mathbb{X}_{\mathcal{J}} \subset \mathbb{X}} \mathbf{f}(\mathbf{x}) \quad (6)$$

subject to *preference-order constraints*. Specifically, we want to explore only that subset of solutions $\mathbb{X}_{\mathcal{J}} \subset \mathbb{X}$ that place more *importance* on one objective f_{i_0} than objective f_{i_1} , and so on, as specified by the (ordered) preference tuple $\mathcal{J} = (i_0, i_1, \dots, i_Q | \{i_0, i_1, \dots\} \subset \mathbb{Z}_m, i_k \neq i_{k'} \forall k \neq k')$, where $Q \in \mathbb{Z}_m$ is the number of defined preferences over objectives.

4.1 Preference-Order Constraints

Let $\mathbf{x}^* \in \operatorname{int}(\mathbb{X}) \cap \mathbb{X}^*$ be a Pareto-optimal point in the interior of \mathbb{X} . Necessary (but not sufficient, local) Pareto optimality conditions require that, for all sufficiently small $\delta \mathbf{x} \in \mathbb{R}^n$, $f(\mathbf{x}^* + \delta \mathbf{x}) \not\prec f(\mathbf{x}^*)$, or, equivalently $(\delta \mathbf{x}^T \nabla_{\mathbf{x}}) \mathbf{f}(\mathbf{x}^*) \notin \mathbb{R}_+^m$. A necessary (again not sufficient) equivalent condition is that, for each axis $j \in \mathbb{Z}_n$ in design space, sufficiently small changes in x_j do not cause all objectives to simultaneously increase (and/or remain unchanged) or decrease (and/or remain unchanged). Failure of this condition would indicate that simply changing design parameter x_j could improve all objectives, and hence that \mathbf{x}^* was not in fact Pareto optimal. In summary, local Pareto optimality requires that $\forall j \in \mathbb{Z}_n$ there exists $\mathbf{s}_{(j)} \in \mathbb{R}_+^m \setminus \{\mathbf{0}\}$ such that:

$$\mathbf{s}_{(j)}^T \frac{\partial}{\partial x_j} \mathbf{f}(\mathbf{x}) = 0 \quad (7)$$

It is important to note that this is not the same as the optimality conditions that may be derived from linear scalarisation, as the optimality conditions that arise from linear scalarisation additionally require that $\mathbf{s}_{(0)} = \mathbf{s}_{(1)} = \dots = \mathbf{s}_{(n-1)}$. Moreover (7) applies to all Pareto-optimal points, whereas linear scalarisation optimisation conditions fail for Pareto points on non-convex regions [29].

Definition 1 (Preference-Order Constraints) Let $\mathcal{J} = (i_0, i_1, \dots, i_Q | \{i_0, i_1, \dots\} \subset \mathbb{Z}_m, i_k \neq i_{k'} \forall k \neq k')$ be an (ordered) preference tuple. A vector $\mathbf{x} \in \mathbb{X}$ satisfies the associated preference-order constraint if $\exists \mathbf{s}_{(0)}, \mathbf{s}_{(1)}, \dots, \mathbf{s}_{(n-1)} \in \mathbb{S}_{\mathcal{J}}$ such that:

$$\mathbf{s}_{(j)}^T \frac{\partial}{\partial x_j} \mathbf{f}(\mathbf{x}) = 0 \quad \forall j \in \mathbb{Z}_n$$

where $\mathbb{S}_{\mathcal{J}} \triangleq \{\mathbf{s} \in \mathbb{R}_+^m \setminus \{\mathbf{0}\} | s_{i_0} \geq s_{i_1} \geq s_{i_2} \geq \dots\}$. Further we define $\mathbb{X}_{\mathcal{J}}$ to be the set of all $\mathbf{x} \in \mathbb{X}$ satisfying the preference-order constraint. Equivalently:

$$\mathbb{X}_{\mathcal{J}} = \{\mathbf{x} \in \mathbb{X} | \frac{\partial}{\partial x_j} \mathbf{f}(\mathbf{x}) \in \mathbb{S}_{\mathcal{J}}^\perp \quad \forall j \in \mathbb{Z}_n\}$$

where $\mathbb{S}_{\mathcal{J}}^\perp \triangleq \{\mathbf{x} \in \mathbb{X} | \exists \mathbf{s} \in \mathbb{S}_{\mathcal{J}}, \mathbf{s}^T \mathbf{x} = 0\}$.

It is noteworthy to mention that (7) and Definition 1 are the key for calculating the compliance of a recommended solution with the preference-order constraints. Having defined preference-order constraints we then calculate the posterior probability that $\mathbf{x} \in \mathbb{X}_{\mathcal{J}}$, and showing how these posterior probabilities may be incorporated into the EHI acquisition function to steer the Bayesian optimiser toward Pareto optimal points that satisfy the preference-order constraint. Before proceeding, however, it is necessary to briefly consider the geometry of $\mathbb{S}_{\mathcal{J}}$ and $\mathbb{S}_{\mathcal{J}}^\perp$.

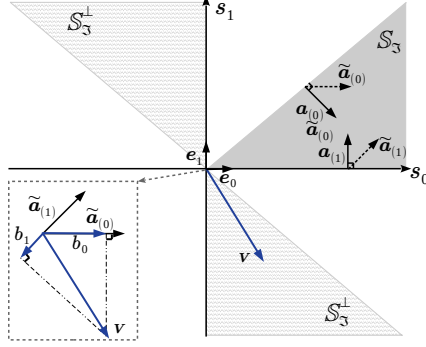


Figure 2: Illustration of $\mathbb{S}_{\mathcal{J}}^{\perp}$, $\mathbb{S}_{\mathcal{J}}$ and the vectors $\mathbf{a}_{(0)}$, $\mathbf{a}_{(1)}$ for a 2D case where $\mathcal{J} = (0, 1)$, so $s_0 > s_1$, $\mathbb{S}_{\mathcal{J}}$ is a proper cone representing the preference-order constraints; $\mathbb{S}_{\mathcal{J}}^{\perp}$ is the union of two sub-spaces. $\mathbf{v} \in \mathbb{S}_{\mathcal{J}}^{\perp}$ implies a solution complying with preference-order constraints. b_0 and b_1 are the projection of \mathbf{v} over $\tilde{\mathbf{a}}_{(0)}$ and $\tilde{\mathbf{a}}_{(1)}$. In order to satisfy $\mathbf{v} \in \mathbb{S}_{\mathcal{J}}$, it is necessary that $\exists \mathbf{s} \in \mathbb{S}_{\mathcal{J}}$ s.t. $\mathbf{v}^T \mathbf{s} = 0$ or equivalently $\mathbf{v} = \mathbf{0}$ or $b_0 = \tilde{\mathbf{a}}_{(0)}^T \mathbf{v}$ and $b_1 = \tilde{\mathbf{a}}_{(1)}^T \mathbf{v}$ have different signs.

4.2 The Geometry of $\mathbb{S}_{\mathcal{J}}$ and $\mathbb{S}_{\mathcal{J}}^{\perp}$

In the following we assume, w.l.o.g, that the preference-order constraints follows the order of indices in objective functions (reorder, otherwise), and that there is at least one constraint.

We now define the preference-order constraints by assumption $\mathcal{J} = (0, 1, \dots, Q | Q \in \mathbb{Z}_m \setminus \{0\})$, where $Q > 0$. This defines the sets $\mathbb{S}_{\mathcal{J}}$ and $\mathbb{S}_{\mathcal{J}}^{\perp}$, which in turn define the constraints that must be met by the gradients of $\mathbf{f}(\mathbf{x})$ - either $\exists \mathbf{s}_{(0)}, \mathbf{s}_{(1)}, \dots, \mathbf{s}_{(n-1)} \in \mathbb{S}_{\mathcal{J}}$ such that $\mathbf{s}_{(j)}^T \frac{\partial}{\partial x_j} \mathbf{f}(\mathbf{x}) = 0 \forall j \in \mathbb{Z}_n$ or, equivalently $\frac{\partial}{\partial x_j} \mathbf{f}(\mathbf{x}) \in \mathbb{S}_{\mathcal{J}}^{\perp} \forall j \in \mathbb{Z}_n$. Next, Theorem 2 defines the representation of $\mathbb{S}_{\mathcal{J}}$.

Theorem 1 *Let $\mathcal{J} = (0, 1, \dots, Q | Q \in \mathbb{Z}_m \setminus \{0\})$ be an (ordered) preference tuple. Define $\mathbb{S}_{\mathcal{J}}$ as per definition 1. Then $\mathbb{S}_{\mathcal{J}}$ is a polyhedral (finitely-generated) proper cone (excluding the origin) that may be represented using either a polyhedral representation:*

$$\mathbb{S}_{\mathcal{J}} = \left\{ \mathbf{s} \in \mathbb{R}^m \mid \mathbf{a}_{(i)}^T \mathbf{s} \geq 0 \forall i \in \mathbb{Z}_m \right\} \setminus \{\mathbf{0}\} \quad (8)$$

or a generative representation:

$$\mathbb{S}_{\mathcal{J}} = \left\{ \sum_{i \in \mathbb{Z}_m} c_i \tilde{\mathbf{a}}_{(i)} \mid \mathbf{c} \in \bar{\mathbb{R}}_+^m \right\} \setminus \{\mathbf{0}\} \quad (9)$$

where $\forall i \in \mathbb{Z}_m$:

$$\mathbf{a}_{(i)} = \begin{cases} \frac{1}{\sqrt{2}} (\mathbf{e}_i - \mathbf{e}_{i+1}) & \text{if } i \in \mathbb{Z}_Q \\ \mathbf{e}_i & \text{otherwise} \end{cases}$$

$$\tilde{\mathbf{a}}_{(i)} = \begin{cases} \frac{1}{\sqrt{i+1}} \sum_{l \in \mathbb{Z}_{i+1}} \mathbf{e}_l & \text{if } i \in \mathbb{Z}_{Q+1} \\ \mathbf{e}_i & \text{otherwise} \end{cases}$$

and $\mathbf{e}_0, \mathbf{e}_1, \dots, \mathbf{e}_{m-1}$ are the Euclidean basis of \mathbb{R}^m .

Proof of Theorem 2 is available in the supplementary material. To test if a point satisfies this requirement we need to understand the geometry of the set $\mathbb{S}_{\mathcal{J}}$. The Theorem 2 shows that $\mathbb{S}_{\mathcal{J}} \cup \{\mathbf{0}\}$ is a polyhedral (finitely generated) proper cone, represented either in terms of half-space constraints (polyhedral form) or as a positive span of extreme directions (generative representation). The geometrical intuition for this is given in Figure 2 for a simple, 2-objective case with a single preference order constraint.

Algorithm 1 Test if $\mathbf{v} \in \mathbb{S}_{\mathcal{J}}^{\perp}$.

Input: Preference tuple \mathcal{J}
Test vector $\mathbf{v} \in \mathbb{R}^m$.
Output: $\mathbb{1}(\mathbf{v} \in \mathbb{S}_{\mathcal{J}}^{\perp})$.
// Calculate $\mathbf{1}(\mathbf{v} \in \mathbb{S}_{\mathcal{J}}^{\perp})$.
Let $b_j = \tilde{\mathbf{a}}_{(j)}^T \mathbf{v} \forall j \in \mathbb{Z}_m$.
if $\exists i \neq k \in \mathbb{Z}_m : \text{sgn}(b_i) \neq \text{sgn}(b_k)$ return
TRUE
elseif $\mathbf{b} = \mathbf{0}$ return TRUE
else return FALSE.

Algorithm 3 Calculate $\Pr(\mathbf{x} \in \mathbb{X}_{\mathcal{J}} | \mathbb{D})$.

Input: Observations $\mathbb{D} = \{(\mathbf{x}_{(i)}, \mathbf{y}_{(i)}) \in \mathbb{X} \times \mathbb{Y}\}$.
Number of Monte Carlo samples R .
Test vector $\mathbf{x} \in \mathbb{X}$.
Output: $\Pr(\mathbf{x} \in \mathbb{X}_{\mathcal{J}} | \mathbb{D})$.
Let $q = 0$.
for $k = 0, 1, \dots, R - 1$ **do**
//Construct samples
 $\mathbf{v}_{(0)}, \mathbf{v}_{(1)}, \dots, \mathbf{v}_{(n-1)} \in \mathbb{R}^m$.
Let $\mathbf{v}_{(j)} = \mathbf{0} \forall j \in \mathbb{Z}_n$.
for $i = 0, 1, \dots, m - 1$ **do**
Sample $\mathbf{u} \sim \mathcal{N}(\boldsymbol{\mu}'_{\mathbb{D}_i}(\mathbf{x}), \boldsymbol{\sigma}'_{\mathbb{D}_i}(\mathbf{x}, \mathbf{x}))$
(see (3)).
Let $[v_{(0)i}, v_{(1)i}, \dots, v_{(n-1)i}] := \mathbf{u}^T$.
end for
//Test if $\mathbf{v}_{(j)} \in \mathbb{S}_{\mathcal{J}}^{\perp} \forall j \in \mathbb{Z}_n$.
Let $q := q + \prod_{j \in \mathbb{Z}_n} \mathbb{1}(\mathbf{v}_{(j)} \in \mathbb{S}_{\mathcal{J}}^{\perp})$ (see algo
rithm 1).
end for
Return $\frac{q}{R}$.

Algorithm 2 Preference-Order Constrained Bayesian Optimisation (MOBO-PC).

Input: preference-order tuple \mathcal{J} .
Observations $\mathbb{D} = \{(\mathbf{x}_{(i)}, \mathbf{y}_{(i)}) \in \mathbb{X} \times \mathbb{Y}\}$.
for $t = 0, 1, \dots, T - 1$ **do**
Select the test point:
 $\mathbf{x} = \underset{\mathbf{x} \in \mathbb{X}}{\text{argmax}} a_t^{\text{PEHI}}(\mathbf{x} | \mathbb{D}_t)$.
(a_t^{PEHI} is evaluated using algorithm 4).
Perform Experiment $\mathbf{y} = \mathbf{f}(\mathbf{x}) + \epsilon$.
Update $\mathbb{D}_{t+1} := \mathbb{D}_t \cup \{(\mathbf{x}, \mathbf{y})\}$.
end for

Algorithm 4 Calculate $a_t^{\text{PEHI}}(\mathbf{x} | \mathbb{D})$.

Input: Observations $\mathbb{D} = \{(\mathbf{x}_{(i)}, \mathbf{y}_{(i)}) \in \mathbb{X} \times \mathbb{Y}\}$.
Number of Monte Carlo samples \tilde{R} .
Test vector $\mathbf{x} \in \mathbb{X}$.
Output: $a_t^{\text{PEHI}}(\mathbf{x} | \mathbb{D})$.
Using algorithm 3, calculate:
 $s_x = \Pr(\mathbf{x} \in \mathbb{X}_{\mathcal{J}} | \mathbb{D})$
 $s_{(j)} = \Pr(\mathbf{x}_{(j)} \in \mathbb{X}_{\mathcal{J}} | \mathbb{D}) \forall (\mathbf{x}_{(j)}, \mathbf{y}_{(j)}) \in \mathbb{D}$
Let $q = 0$.
for $k = 0, 1, \dots, \tilde{R} - 1$ **do**
Sample $y_i \sim \mathcal{N}(\mu_{\mathbb{D}_i}(\mathbf{x}), \sigma_{\mathbb{D}_i}(\mathbf{x})) \forall i \in \mathbb{Z}_m$ (see (2)).
Construct cells c_0, c_1, \dots from $\mathbb{D} \cup \{(\mathbf{x}, \mathbf{y})\}$ by sorting along each axis in objective space to form a grid.
Calculate:
 $q = q +$
 $s_x \sum_{k: \mathbf{y} \succeq \tilde{\mathbf{y}}_{c_k}} \text{vol}(c_k) \prod_{j \in \mathbb{Z}_N: \mathbf{y}_{(j)} \succeq \tilde{\mathbf{y}}_{c_k}} (1 - s_{(j)})$
end for
Return q / \tilde{R} .

The subsequent corollary allows us to construct a simple algorithm (algorithm 1) to test if a vector \mathbf{v} lies in the set $\mathbb{S}_{\mathcal{J}}^{\perp}$. We will use this algorithm to test if $\frac{\partial}{\partial x_j} \mathbf{f}(\mathbf{x}) \in \mathbb{S}_{\mathcal{J}}^{\perp} \forall j \in \mathbb{Z}_n$ - that is, if \mathbf{x} satisfies the preference-order constraints. The proof of corollary 2 is available in the supplementary material.

Corollary 1 Let $\mathcal{J} = (0, 1, \dots, Q | Q \in \mathbb{Z}_m \setminus \{0\})$ be an (ordered) preference tuple. Define $\mathbb{S}_{\mathcal{J}}^{\perp}$ as per definition 1. Using the notation of Theorem 2, $\mathbf{v} \in \mathbb{S}_{\mathcal{J}}^{\perp}$ if and only if $\mathbf{v} = \mathbf{0}$ or $\exists i \neq k \in \mathbb{Z}_m$ such that $\text{sgn}(\tilde{\mathbf{a}}_{(i)}^T \mathbf{v}) \neq \text{sgn}(\tilde{\mathbf{a}}_{(k)}^T \mathbf{v})$, where $\text{sgn}(0) = 0$.

5 Preference Constrained Bayesian Optimisation

In this section we do two things. First, we show how the Gaussian process models of the objectives f_i (and their derivatives) may be used to calculate the posterior probability that $\mathbf{x} \in \mathbb{X}_{\mathcal{J}}$ defined by $\mathcal{J} = (0, 1, \dots, Q | Q \in \mathbb{Z}_m \setminus \{0\})$. Second, we show how the EHI acquisition function may be modified and calculated to incorporate these probabilities and hence only reward points that satisfy the preference-order conditions. Finally, we give our algorithm using this acquisition function.

5.1 Calculating Posterior Probabilities

Given that $f_i \sim \mathcal{GP}(0, K_{(i)}(\mathbf{x}, \mathbf{x}))$ are draws from independent Gaussian processes, and given observations \mathbb{D} , we wish to calculate the posterior probability that $\mathbf{x} \in \mathbb{X}_{\mathcal{J}}$ -

i.e.: $\Pr(\mathbf{x} \in \mathbb{X}_{\mathcal{J}} | \mathbb{D}) = \Pr\left(\frac{\partial}{\partial \mathbf{x}_j} \mathbf{f}(\mathbf{x}) \in \mathbb{S}_{\mathcal{J}}^{\perp} \forall j \in \mathbb{Z}_n\right)$. As $f_i \sim \mathcal{GP}(0, K_{(i)}(\mathbf{x}, \mathbf{x}))$ it follows that $\nabla_{\mathbf{x}} f_i(\mathbf{x}) | \mathbb{D} \sim \mathcal{N}_i \triangleq \mathcal{N}(\boldsymbol{\mu}'_{\mathbb{D}i}(\mathbf{x}), \boldsymbol{\sigma}'_{\mathbb{D}i}(\mathbf{x}, \mathbf{x}'))$, as defined by (3). Hence:

$$\Pr(\mathbf{x} \in \mathbb{X}_{\mathcal{J}} | \mathbb{D}) = \Pr\left(\mathbf{v}^{(j)} \in \mathbb{S}_{\mathcal{J}}^{\perp} \left| \begin{array}{c} v_{(0)i} \\ v_{(1)i} \\ \vdots \\ v_{(n-1)i} \end{array} \right. \sim \mathcal{N}_i \forall i \in \mathbb{Z}_m\right)$$

where $\mathbf{v} \sim P(\nabla_{\mathbf{x}} \mathbf{f} | \mathbb{D})$. We estimate it using Monte-Carlo [7] sampling as per algorithm 3.

5.2 Preference-Order Constrained Bayesian Optimisation Algorithm (MOBO-PC)

Our complete Bayesian optimisation algorithm with Preference-order constraints is given in algorithm 2. The acquisition function introduced in this algorithm gives higher importance to points satisfying the preference-order constraints. Unlike standard EHI, we take expectation over both the expected experimental outcomes $f_i(\mathbf{x}) \sim \mathcal{N}(\mu_{\mathbb{D}i}(\mathbf{x}), \sigma_{\mathbb{D}i}(\mathbf{x}, \mathbf{x}))$, $\forall i \in \mathbb{Z}_m$, and the probability that points $\mathbf{x}_{(i)} \in \mathbb{X}_{\mathcal{J}}$ and $\mathbf{x} \in \mathbb{X}_{\mathcal{J}}$ satisfy the preference-order constraints. We define our preference-based EHI acquisition function as:

$$a_t^{\text{PEHI}}(\mathbf{x} | \mathbb{D}) = \mathbb{E}[S_{\mathcal{J}}(\mathbb{D} \cup \{(\mathbf{x}, \mathbf{f}(\mathbf{x}))\}) - S_{\mathcal{J}}(\mathbb{D}) | \mathbb{D}] \quad (10)$$

where $S_{\mathcal{J}}(\mathbb{D})$ is the hypervolume dominated by the observations $(\mathbf{x}, \mathbf{y}) \in \mathbb{D}$ satisfying the preference-order constraints. The calculation of $S_{\mathcal{J}}(\mathbb{D})$ is illustrated in the supplementary material. The expectation of $S_{\mathcal{J}}(\mathbb{D})$ given \mathbb{D} is:

$$\begin{aligned} \mathbb{E}[S_{\mathcal{J}}(\mathbb{D}) | \mathbb{D}] &= \sum_k \text{vol}(c_k) \Pr(\exists (\mathbf{x}, \mathbf{y}) \in \mathbb{D} | \mathbf{y} \succeq \tilde{\mathbf{y}}_{c_k} \wedge \dots \mathbf{x} \in \mathbb{X}_{\mathcal{J}}) \dots \\ &= \sum_k \text{vol}(c_k) \left(1 - \prod_{(\mathbf{x}, \mathbf{y}) \in \mathbb{D}: \mathbf{y} \succeq \tilde{\mathbf{y}}_{c_k}} (1 - \Pr(\mathbf{x} \in \mathbb{X}_{\mathcal{J}} | \mathbb{D}))\right) \end{aligned}$$

where $\tilde{\mathbf{y}}_{c_k}$ is the dominant corner of cell c_k , $\text{vol}(c_k)$ is the hypervolume of cell c_k , and the cells c_k are constructed by sorting \mathbb{D} along each axis in objective space. The posterior probabilities $\Pr(\mathbf{x} \in \mathbb{X}_{\mathcal{J}} | \mathbb{D})$ are calculated using algorithm 3. It follows that:

$$a_t^{\text{PEHI}}(\mathbf{x} | \mathbb{D}) = \Pr(\mathbf{x} \in \mathbb{X}_{\mathcal{J}} | \mathbb{D}) \mathbb{E}\left[\sum_{k: \mathbf{y} \succeq \tilde{\mathbf{y}}_{c_k}} \text{vol}(c_k) \prod_{j \in \mathbb{Z}_N: \mathbf{y}^{(j)} \succeq \tilde{\mathbf{y}}_{c_k}} (1 - \Pr(\mathbf{x}_{(j)} \in \mathbb{X}_{\mathcal{J}} | \mathbb{D})) \mid y_i \sim \dots \mathcal{N}(\mu_{\mathbb{D}i}(\mathbf{x}), \sigma_{\mathbb{D}i}(\mathbf{x})) \forall i \in \mathbb{Z}_m\right]$$

where the cells c_k are constructed using the set $\mathbb{D} \cup \{(\mathbf{x}, \mathbf{y})\}$ by sorting along the axis in objective space. We estimate this acquisition function using Monte-Carlo simulation shown in algorithm 4.

6 Experiments

We conduct a series of experiments to test the empirical performance of our proposed method MOBO-PC and compare with other strategies. These experiments including synthetic data as well as optimizing the hyper-parameters of a feed-forward neural network. For Gaussian process, we use maximum likelihood estimation for setting hyperparameters [22].

6.1 Baselines

To the best of our knowledge there are no studies aiming to solve our proposed problem, however we are using PESMO, SMSego, SUR, ParEGO and EHI [10, 21, 20, 15, 8] to confirm the validity of the obtained Pareto front solutions. The obtained Pareto front must be in the ground-truth whilst also satisfying the preference-order constraints. We compare our results with MOBO-RS [19] by suitably specifying bounding boxes in the objective space that can replicate a preference-order constraint.

6.2 Synthetic Functions

We begin with a comparison on minimising synthetic function Schaffer function N. 1 with 2 conflicting objectives f_0, f_1 and 1-dimensional input. (see [25]). Figure 3a shows the ground-truth Pareto front

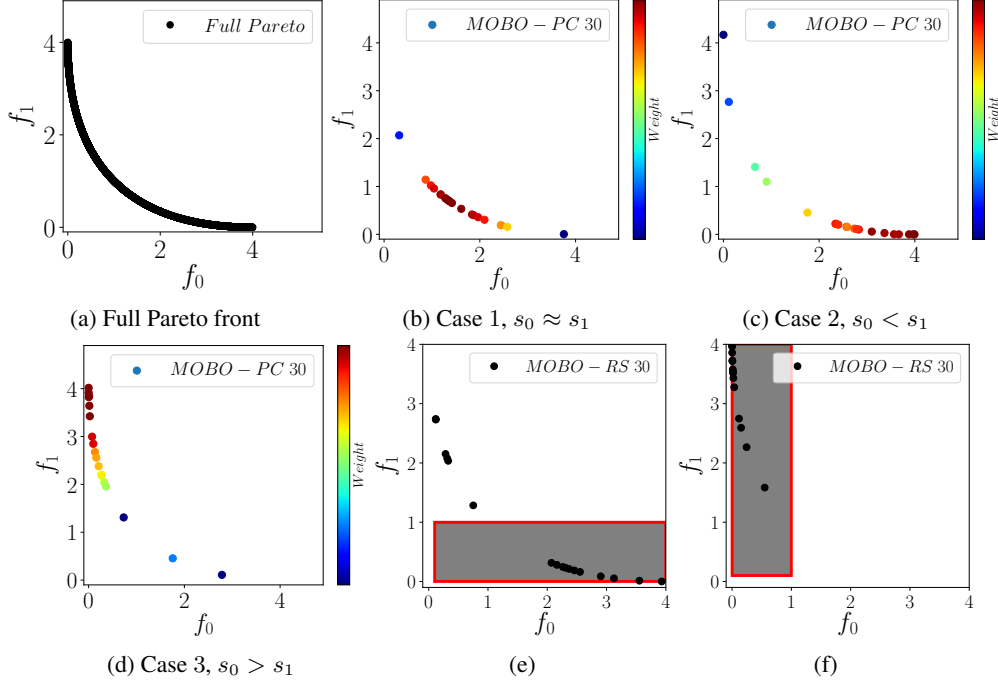


Figure 3: Finding Pareto front which comply with the preference-order constraint. Figure 3a shows the full Pareto front solution (with no preferences). Figure 3b illustrates the Pareto front by assuming stability of first objective f_0 is similar to second objective f_1 . In Figure 3c, stability of f_1 is preferred over f_0 . Figure 3d shows more stable results for f_0 than f_1 ($s_0 > s_1$). Figure 3e and 3f shows the results obtained by MOBO-RS and the corresponding bounding boxes. The gradient color of the Pareto front points in Figure 3b-3d indicates their degree of compliance with the constraints.

for this function. To illustrate the behavior of our method, we impose distinct preferences. Three test cases are designed to illustrate the effects of imposing preference-order constraints on the objective functions for stability. Case (1): $s_0 \approx s_1$, Case (2): $s_0 < s_1$ and Case (3): $s_0 > s_1$. For our method it is only required to define the preference-order constraints, however for MOBO-RS, additional information as a bounding box is obligatory. Figure 3b (case 1), shows the results of preference-order constraints $\mathbb{S}_\gamma \triangleq \{\mathbf{s} \in \mathbb{R}_+^m \setminus \{\mathbf{0}\} \mid s_0 \approx s_1\}$ for our proposed method, where s_0 represents the importance of stability in minimising f_0 and s_1 is the importance of stability in minimising f_1 . Due to same importance of both objectives, a balanced optimisation is expected. Higher weights are obtained for the Pareto front points in the middle region with highest stability for both objectives. Figure 3c (case 2) is based on the preference-order of $s_0 < s_1$ that implies the importance of stability in f_1 is more than f_0 . The results show more stable Pareto points for f_1 than f_0 . Figure 3d (case 3) shows the results of $s_0 > s_1$ preference-order constraint. As expected, we see more number of stable Pareto points for the important objective (i.e. f_0 in this case). We defined two bounding boxes for MOBO-RS approach which can represent the preference-order constraints in our approach (Figure 3e and 3f). There are infinite possible bounding boxes can serve as constraints on objectives in such problems, consequently, the instability of results is expected across the various definitions of bounding boxes. We believe our method can obtain more stable Pareto front solutions especially when prior information is sparse. Also, having extra information as the weight (importance) of the Pareto front points is another advantage.

Figure 4 illustrates a special test case in which $s_0 > s_1$ and $s_2 > s_1$, yet no preferences specified over f_2 and f_0 while minimising Viennet function. The proposed complex preference-order constraint does not form a proper cone as elaborated in Theorem 2. However, $s_0 > s_1$ independently constructs a proper cone, likewise for $s_2 > s_1$. Figure 4a shows the results of processing these two independent constraints separately, merging their results and finding the Pareto front. Figure 4b implies more stable solutions for f_0 comparing to f_1 . Figure 4c shows the Pareto front points comply with $s_2 > s_1$.

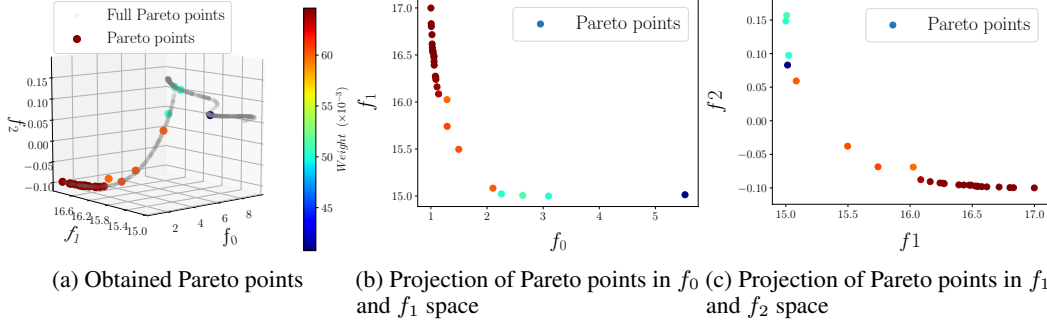


Figure 4: Finding Pareto front points with partial constraints as specified by $s_0 > s_1$ and $s_2 > s_1$. Figure 4a shows the 3D plot of the obtained Pareto front points satisfying preference-order constraints with the color indicating the degree of compliance. Figure 4b illustrates the projection of Pareto optimal points on $f_0 \times f_1$ sub-space, and figure 4c shows the projection on $f_1 \times f_2$ sub-space.

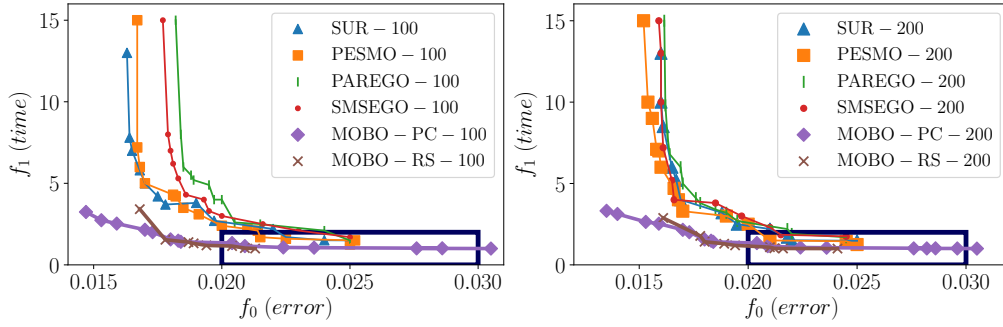


Figure 5: Average Pareto fronts obtained by proposed method in comparison to other methods. This experiment defines $s_1 > s_0$ i.e. stability of run time is more important than the error. For MOBO-RS, $[[0.02, 0], [0.03, 2]]$ is an additional information used as bounding box. The other methods do not incorporate preferences. The results are shown for 100 evaluations of the objectives (left) and 200 evaluations of the objectives (right).

6.3 Finding a Fast and Accurate Neural Network

Next, we train a neural network with two objectives of minimising both prediction error and prediction time, as per [10]. These are conflicting objectives because reducing the prediction error generally involves larger networks and consequently longer testing time. We are using MNIST dataset and the tuning parameters include number of hidden layers ($x_1 \in [1, 3]$), the number of hidden units per layer ($x_2 \in [50, 300]$), the learning rate ($x_3 \in (0, 0.2]$), amount of dropout ($x_4 \in [0.4, 0.8]$), and the level of l_1 ($x_5 \in (0, 0.1]$) and l_2 ($x_6 \in (0, 0.1]$) regularization. For this problem we assume stability of $f_1(\text{time})$ in minimising procedure is more important than the $f_0(\text{error})$. For MOBO-RS method, we selected $[[0.02, 0], [0.03, 2]]$ bounding box to represent an accurate prior knowledge (see Figure 5). The results were averaged over 5 independent runs. Figure 5 illustrates that one can simply ask for more stable solutions with respect to test time (without any prior knowledge) of a neural network while optimising the hyperparameters. As all the solutions found with MOBO-PC are in range of (0, 5) test time. In addition, it seems the proposed method finds more number of Pareto front solutions in comparison with MOBO-RS.

7 Conclusion

In this paper we proposed a novel multi-objective Bayesian optimisation algorithm with preferences over objectives. We define objective preferences in terms of stability and formulate a common framework to focus on the sections of the Pareto front where preferred objectives are more stable, as is required. We evaluate our method on both synthetic and real-world problems and show that the obtained Pareto fronts comply with the preference-order constraints.

Acknowledgments

This research was partially funded by Australian Government through the Australian Research Council (ARC). Prof Venkatesh is the recipient of an ARC Australian Laureate Fellowship (FL170100006).

References

- [1] Roberto Calandra, Nakul Gopalan, André Seyfarth, Jan Peters, and Marc Peter Deisenroth. Bayesian gait optimization for bipedal locomotion. In *International Conference on Learning and Intelligent Optimization*, pages 274–290. Springer, 2014.
- [2] Roberto Calandra, André Seyfarth, Jan Peters, and Marc Peter Deisenroth. Bayesian optimization for learning gaits under uncertainty. *Annals of Mathematics and Artificial Intelligence*, 76(1-2):5–23, 2016.
- [3] Kalyanmoy Deb. Multi-objective optimization. In *Search methodologies*, pages 273–316. Springer, 2005.
- [4] Kalyanmoy Deb. Multi-objective optimization. In *Search methodologies*, pages 403–449. Springer, 2014.
- [5] Kalyanmoy Deb, Samir Agrawal, Amrit Pratap, and Tanaka Meyarivan. A fast elitist non-dominated sorting genetic algorithm for multi-objective optimization: Nsga-ii. In *International conference on parallel problem solving from nature*, pages 849–858. Springer, 2000.
- [6] Kalyanmoy Deb, Lothar Thiele, Marco Laumanns, and Eckart Zitzler. Scalable multi-objective optimization test problems. In *Proceedings of the 2002 Congress on Evolutionary Computation. CEC’02 (Cat. No. 02TH8600)*, volume 1, pages 825–830. IEEE, 2002.
- [7] Pierre Del Moral, Arnaud Doucet, and Ajay Jasra. Sequential monte carlo samplers. *Journal of the Royal Statistical Society: Series B (Statistical Methodology)*, 68(3):411–436, 2006.
- [8] Michael Emmerich and Jan-willem Klinkenberg. The computation of the expected improvement in dominated hypervolume of pareto front approximations. *Rapport technique, Leiden University*, 34, 2008.
- [9] Paul Feliot, Julien Bect, and Emmanuel Vazquez. A bayesian approach to constrained single- and multi-objective optimization. *Journal of Global Optimization*, 67(1-2):97–133, 2017.
- [10] Daniel Hernández-Lobato, Jose Hernandez-Lobato, Amar Shah, and Ryan Adams. Predictive entropy search for multi-objective bayesian optimization. In *International Conference on Machine Learning*, pages 1492–1501, 2016.
- [11] Simon Huband, Phil Hingston, Lyndon While, and Luigi Barone. An evolution strategy with probabilistic mutation for multi-objective optimisation. In *Proceedings of the IEEE Congress on Evolutionary Computation*, volume 4, pages 2284–2291, 2003.
- [12] Iris Hupkens, André Deutz, Kaifeng Yang, and Michael Emmerich. Faster exact algorithms for computing expected hypervolume improvement. In *International Conference on Evolutionary Multi-Criterion Optimization*, pages 65–79. Springer, 2015.
- [13] Ilija Ilievski, Taimoor Akhtar, Jiashi Feng, and Christine Annette Shoemaker. Efficient hyperparameter optimization for deep learning algorithms using deterministic rbf surrogates. In *Thirty-First AAAI Conference on Artificial Intelligence*, 2017.
- [14] Aaron Klein, Stefan Falkner, Simon Bartels, Philipp Hennig, and Frank Hutter. Fast bayesian optimization of machine learning hyperparameters on large datasets. *arXiv preprint arXiv:1605.07079*, 2016.
- [15] Joshua Knowles. Parego: a hybrid algorithm with on-line landscape approximation for expensive multiobjective optimization problems. *IEEE Transactions on Evolutionary Computation*, 10(1):50–66, 2006.
- [16] Marco Laumanns and Jiri Ocenasek. Bayesian optimization algorithms for multi-objective optimization. In *International Conference on Parallel Problem Solving from Nature*, pages 298–307. Springer, 2002.
- [17] Cheng Li, David Rubín de Celis Leal, Santu Rana, Sunil Gupta, Alessandra Sutti, Stewart Greenhill, Teo Slezak, Murray Height, and Svetha Venkatesh. Rapid bayesian optimisation for synthesis of short polymer fiber materials. *Scientific reports*, 7(1):5683, 2017.

- [18] A. O’Hagan. Some bayesian numerical analysis. *Bayesian Statistics*, 7:345–363, 1992.
- [19] Biswajit Paria, Kirthevasan Kandasamy, and Barnabás Póczos. A flexible multi-objective bayesian optimization approach using random scalarizations. *CoRR*, abs/1805.12168, 2018.
- [20] Victor Picheny. Multiobjective optimization using gaussian process emulators via stepwise uncertainty reduction. *Statistics and Computing*, 25(6):1265–1280, 2015.
- [21] Wolfgang Ponweiser, Tobias Wagner, Dirk Biermann, and Markus Vincze. Multiobjective optimization on a limited budget of evaluations using model-assisted s-metric selection. In *International Conference on Parallel Problem Solving from Nature*, pages 784–794. Springer, 2008.
- [22] Carl Edward Rasmussen. Gaussian processes in machine learning. In *Advanced lectures on machine learning*, pages 63–71. Springer, 2004.
- [23] Carl Edward Rasmussen. Gaussian processes to speed up hybrid monte carlo for expensive bayesian integrals. *Bayesian statistics*, 7:651–659, 2008.
- [24] Carl Edward Rasmussen and Christopher K. I. Williams. *Gaussian Processes for Machine Learning*. MIT Press, 2006.
- [25] James David Schaffer. Some experiments in machine learning using vector evaluated genetic algorithms (artificial intelligence, optimization, adaptation, pattern recognition). 1984.
- [26] Alistair Shilton, Santu Rana, Sinil Kumar Gupta, and Svetha Venkatesh. A simple recursive algorithm for calculating expected hypervolume improvement. In *BayesOpt2017 NIPS Workshop on Bayesian Optimisation*, 2017.
- [27] Ofer M. Shir, Michael Emmerich, Thomas Back, and Marc J. J. Vrakking. The application of evolutionary multi-criteria optimization to dynamic molecular alignment. In *Proceedings of 2007 IEEE Congress on Evolutionary Computation*, 2007.
- [28] Jasper Snoek, Hugo Larochelle, and Ryan P Adams. Practical bayesian optimization of machine learning algorithms. In *Advances in neural information processing systems*, pages 2951–2959, 2012.
- [29] Kristof Van Moffaert, Madalina M Drugan, and Ann Nowé. Scalarized multi-objective reinforcement learning: Novel design techniques. In *Adaptive Dynamic Programming and Reinforcement Learning (ADPRL)*, pages 191–199, 2013.
- [30] Lyndon While, Philip Hingston, Luigi Barone, and Simon Huband. A faster algorithm for calculating hypervolume. *IEEE Transactions on Evolutionary Computation*, 10(1):29–38, 2006.
- [31] Martin Zaefferer, Thomax Bartz-Beielstein, Boris Naujoks, Tobias Wagner, and Michael Emmerich. A case study on multi-criteria optimization of an event detection software under limited budgets. In *Proceedings of the 2013 International Conference on Evolutionary Multi-Criterion Optimization*, pages 756–770. Springer, 2013.
- [32] Eckart Zitzler. *Evolutionary Algorithms for Multiobjective Optimization: Methods and Applications*. PhD thesis, Swiss Federal Institute of Technology Zurich, 1999.

Supplementary Materials

8 Method of Evaluation

For a more precise evaluation of our proposed method, we can define a measurement by checking how many of the Pareto front solutions satisfy the preference-order constraints. Based on Algorithm 3, we can calculate the percentage of solutions that satisfy the preference-order constraints by using the gradients of the actual synthetic functions at iteration t . In real-world problems, we may use the gradients of the trained Gaussian Process to evaluate the compliance of Pareto front with preference-order constraints.

It is noteworthy to mention that our function evaluations are expensive, and hence, throwing away evaluations during post-processing is undesirable. Our approach, in contrast, samples such that most of the function evaluations would have desirable characteristics, and hence, would be efficient. Considering Figure 6, given a preference-order constraint as “stability of f_0 being more important than f_1 ” in Schaffer function N. 1, i.e. $\|\frac{\partial f_0}{\partial x}\| \leq \|\frac{\partial f_1}{\partial x}\|$, Figure 6 (a) illustrates the Pareto front obtained by a plain multi-objective optimisation (with no constraints). After the Pareto solutions are found (in 20 iterations), using the derivatives of the trained Gaussian Processes (actual objective functions are black-box), we can post process the obtained Pareto front based on the stability of solutions. Figure 6 (a) shows that only $\frac{6}{18}$ of these solutions have actually met the preference-order constraints. Whereas Figure 6 (b) shows that $\frac{16}{16}$ of the obtained Pareto front solutions by MOBO-PC (in the same 20 iterations) have met the preference-order constraints.

In general, our experimental results show 98.8% of solutions found for Schaffer function N. 1 after 20 iterations comply with constraints. As for Poloni’s two objective function, 86.3% of the solutions follow the constraints after 200 iterations and finally for Viennet 3D function, this number is 82.5%.

Given that the prior knowledge is not provided in [19], the obtained results for their method with same experimental design and the same number of iterations are 47.2% for Schaffer function N. 1, 29.6% for Poloni’s two objective function and 19.3% for Viennet 3D function respectively. This gap explains the importance of the prior knowledge about hyperboxes for their method. The reported numbers are averaged over 10 independent runs. Table 1 summarises the obtained results.

Table 1: Percentage of the Pareto front solutions complying with preference-order constraints in different synthetic functions.

	Schaffer function N. 1	Poloni	Viennet 3D
MOBO-PC	98.8%	86.3%	82.5%
MOBO-RS	47.2%	29.6%	19.3%

9 Proofs

Theorem 2 Let $\mathfrak{J} = (0, 1, \dots, Q | Q \in \mathbb{Z}_m \setminus \{0\})$ be an (ordered) preference tuple. Define $\mathbb{S}_{\mathfrak{J}}$ as per definition 1. Then $\mathbb{S}_{\mathfrak{J}}$ is a polyhedral (finitely-generated) proper cone (excluding the origin) that may be represented using either a polyhedral representation:

$$\mathbb{S}_{\mathfrak{J}} = \left\{ \mathbf{s} \in \mathbb{R}^m \mid \mathbf{a}_{(i)}^T \mathbf{s} \geq 0 \forall i \in \mathbb{Z}_m \right\} \setminus \{0\} \quad (11)$$

or a generative representation:

$$\mathbb{S}_{\mathfrak{J}} = \left\{ \sum_{i \in \mathbb{Z}_m} c_i \tilde{\mathbf{a}}_{(i)} \mid \mathbf{c} \in \bar{\mathbb{R}}_+^m \right\} \setminus \{0\} \quad (12)$$

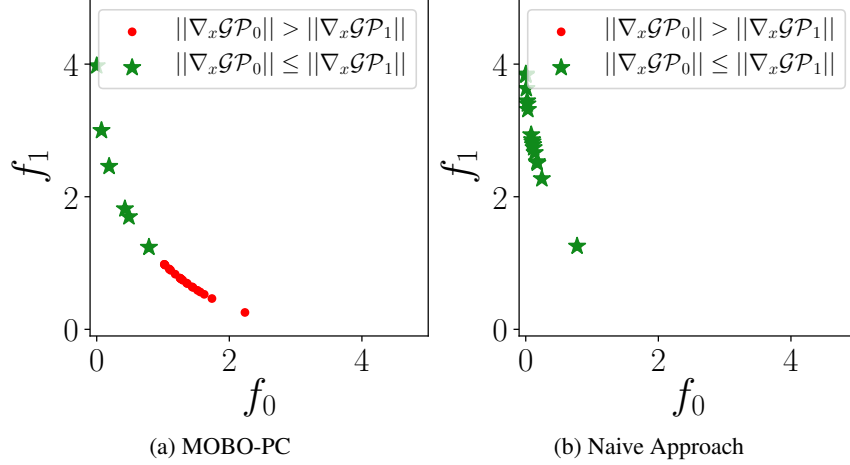


Figure 6: (a) Illustrates a naive approach of post-processing in which almost 50% of the solutions are not complying with preference-order constraints and must be disregarded. (b) Shows an obtained Pareto front by MOBO-PC. All of the obtained solutions are complying with the preference-order constraints based on the derivative of the trained Gaussian Processes.

where $\forall i \in \mathbb{Z}_m$:

$$\mathbf{a}_{(i)} = \begin{cases} \frac{1}{\sqrt{2}} (\mathbf{e}_i - \mathbf{e}_{i+1}) & \text{if } i \in \mathbb{Z}_Q \\ \mathbf{e}_i & \text{otherwise} \end{cases}$$

$$\tilde{\mathbf{a}}_{(i)} = \begin{cases} \frac{1}{\sqrt{i+1}} \sum_{l \in \mathbb{Z}_{i+1}} \mathbf{e}_l & \text{if } i \in \mathbb{Z}_{Q+1} \\ \mathbf{e}_i & \text{otherwise} \end{cases}$$

and $\mathbf{e}_0, \mathbf{e}_1, \dots, \mathbf{e}_{m-1}$ are the Euclidean basis of \mathbb{R}^m .

Proof: The polyhedral representation follows directly from consideration of the constraints $s_i \geq 0$, from which we derive the constraints $\mathbf{a}_{(i)}^T \mathbf{s} = s_i \geq 0 \forall i \notin \mathbb{Z}_Q$; and the constraints $s_k \geq s_{k+1} \forall k \in \mathbb{Z}_Q$, from which we derive the constraints $\mathbf{a}_{(k)}^T \mathbf{s} = s_k - s_{k+1} \geq 0 \forall k = 0, 1, \dots, Q-1$. Moreover $\mathbb{S}_{\mathcal{J}} \cup \{\mathbf{0}\} \subset \mathbb{R}_+^m$ is constructed by restricting \mathbb{R}_+^m using half-space constraints, so $\mathbb{S}_{\mathcal{J}} \cup \{\mathbf{0}\}$ is a proper cone.

The generative representation follows from the fact that a proper conic polyhedra is positively spanned by its extreme directions ($\tilde{\mathbf{a}}_{(i)}$) - i.e. the intersections of the hyperplanes $\mathbf{a}_{(i)}^T \mathbf{s} = 0$. So $\forall i \in \mathbb{Z}_m$, $\tilde{\mathbf{a}}_{(i)}$ must satisfy:

$$\tilde{\mathbf{a}}_{(i)}^T \mathbf{a}_{(j)} = 0 \forall j \neq i \quad (13)$$

There are six cases that are possible combinations of i and j . We show how (13) holds in all the conditions.

1. $i \in \{0, 1, \dots, Q-1\}$ and $j \in \{Q, Q+1, \dots, m-1\}$: considering theorem 2, $\tilde{\mathbf{a}}_{(i)}^T \mathbf{a}_{(j)} = \tilde{\mathbf{a}}_{(i)}^T \mathbf{e}_j = 0$. Therefore $\tilde{\mathbf{a}}_{(i)j} = 0$. Which implies $\tilde{\mathbf{a}}_{(i)Q} = \tilde{\mathbf{a}}_{(i)Q+1} = \dots = \tilde{\mathbf{a}}_{(i)m-1} = 0$.
2. $i \in \{0, 1, \dots, Q-1\}$ and $j \in \{0, 1, \dots, Q-1\} \setminus \{i\}$: based on theorem 2, $\tilde{\mathbf{a}}_{(i)}^T \mathbf{a}_{(j)} = \tilde{\mathbf{a}}_{(i)}^T \frac{1}{\sqrt{2}} (\mathbf{e}_j - \mathbf{e}_{j+1}) = \frac{1}{\sqrt{2}} (\tilde{\mathbf{a}}_{(i)j} - \tilde{\mathbf{a}}_{(i)j+1}) = 0$. Therefore $\tilde{\mathbf{a}}_{(i)j} = \tilde{\mathbf{a}}_{(i)j+1}$. Hence $\tilde{\mathbf{a}}_{(i)0} = \tilde{\mathbf{a}}_{(i)1} = \dots = \tilde{\mathbf{a}}_{(i)i}$ and $\tilde{\mathbf{a}}_{(i)i+1} = \tilde{\mathbf{a}}_{(i)i+2} = \dots = \tilde{\mathbf{a}}_{(i)Q} = 0$. Which results in $\tilde{\mathbf{a}}_{(i)} = \frac{1}{\sqrt{i+1}} \sum_{l \in \mathbb{Z}_{i+1}} \mathbf{e}_l$.
3. $i \in \{Q+1, Q+2, \dots, m-1\}$ and $j \in \{Q, Q+1, \dots, m-1\} \setminus \{i\}$: likewise, $\tilde{\mathbf{a}}_{(i)}^T \mathbf{a}_{(j)} = \tilde{\mathbf{a}}_{(i)}^T \mathbf{e}_j = \tilde{\mathbf{a}}_{(i)j} = 0$. Hence $\tilde{\mathbf{a}}_{(i)Q} = \tilde{\mathbf{a}}_{(i)Q+1} = \dots = \tilde{\mathbf{a}}_{(i)m-1} = 0$, excluding $\tilde{\mathbf{a}}_{(i)i}$, where $\tilde{\mathbf{a}}_{(i)i} \neq 0$ since $j \neq i$.
4. $i \in \{Q+1, Q+2, \dots, m-1\}$ and $j \in \{0, 1, \dots, Q-1\} \setminus \{i\}$: we know $\tilde{\mathbf{a}}_{(i)}^T \mathbf{a}_{(j)} = \tilde{\mathbf{a}}_{(i)}^T \frac{1}{\sqrt{2}} (\mathbf{e}_j - \mathbf{e}_{j+1}) = 0$. Likewise $\tilde{\mathbf{a}}_{(i)0} = \tilde{\mathbf{a}}_{(i)1} = \dots = \tilde{\mathbf{a}}_{(i)Q} = 0$.

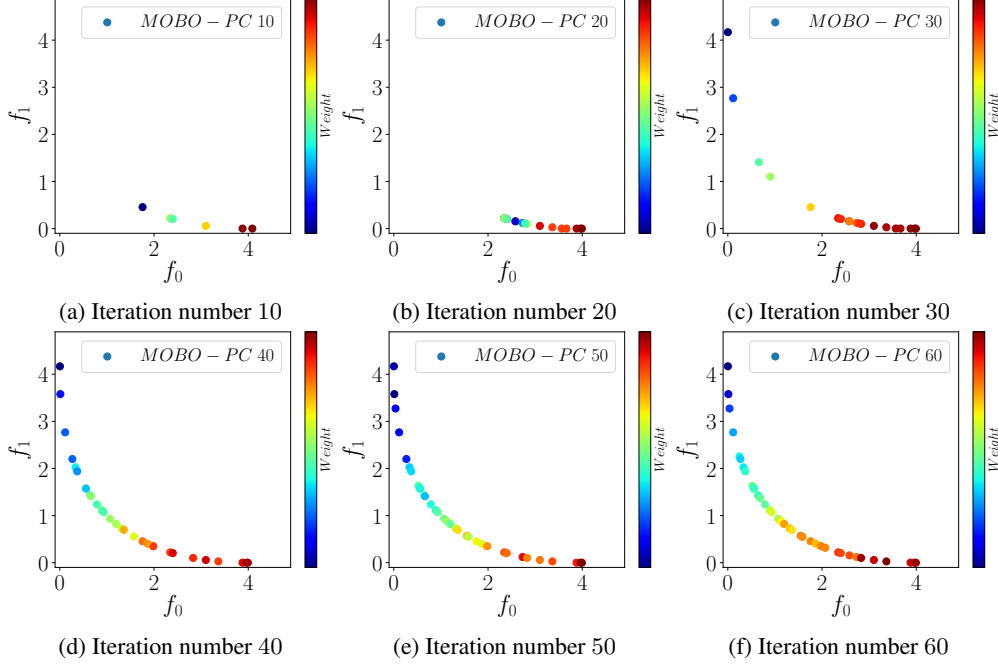


Figure 7: Illustration of the progress of MOBO-PC on Schaffer function N. 1.

5. $i = Q$ and $j \in \{Q + 1, \dots, m - 1\}$: Since $i \neq j$, then $j \in \{Q + 1, Q + 2, \dots, m - 1\}$. Hence $\tilde{\mathbf{a}}_{(i)}^T \mathbf{a}_{(j)} = \tilde{\mathbf{a}}_{(i)}^T \mathbf{e}_j = \tilde{\mathbf{a}}_{(i)j} = 0$. Therefore $\tilde{\mathbf{a}}_{(i)Q+1} = \dots = \tilde{\mathbf{a}}_{(i)m-1} = 0$.
6. $i = Q$ and $j \in \{0, 1, \dots, Q - 1\}$: By defining $i = Q$, we know that $i \neq j$, hence $\tilde{\mathbf{a}}_{(i)}^T \mathbf{a}_{(j)} = \tilde{\mathbf{a}}_{(i)}^T \frac{1}{\sqrt{2}}(\mathbf{e}_j - \mathbf{e}_{j+1}) = \frac{1}{\sqrt{2}}(\tilde{\mathbf{a}}_{(i)j} - \tilde{\mathbf{a}}_{(i)j+1}) = 0$, which implies $\tilde{\mathbf{a}}_{(i)0} = \tilde{\mathbf{a}}_{(i)1} = \dots = \tilde{\mathbf{a}}_{(i)Q}$, or likewise $\tilde{\mathbf{a}}_{(i)} = \frac{1}{\sqrt{Q+1}} \sum_{l \in \mathbb{Z}_{Q+1}} \mathbf{e}_l$.

□

Corollary 2 Let $\mathcal{J} = (0, 1, \dots, Q | Q \in \mathbb{Z}_m \setminus \{0\})$ be an (ordered) preference tuple. Define $\mathbb{S}_{\mathcal{J}}^{\perp}$ as per definition 1. Using the notation of theorem 2, $\mathbf{v} \in \mathbb{S}_{\mathcal{J}}^{\perp}$ if and only if $\mathbf{v} = \mathbf{0}$ or $\exists i \neq k \in \mathbb{Z}_m$ such that $\text{sgn}(\tilde{\mathbf{a}}_{(i)}^T \mathbf{v}) \neq \text{sgn}(\tilde{\mathbf{a}}_{(k)}^T \mathbf{v})$, where $\text{sgn}(0) = 0$.

Proof: By definition of $\mathbb{S}_{\mathcal{J}}^{\perp}$, $\mathbf{v} \in \mathbb{S}_{\mathcal{J}}^{\perp}$ if $\exists \mathbf{s} \in \mathbb{S}_{\mathcal{J}}$ such that $\mathbf{s}^T \mathbf{v} = 0$. This is trivially true of $\mathbf{v} = \mathbf{0}$. Otherwise, using the generative representation of $\mathbb{S}_{\mathcal{J}}$, there must exist $\mathbf{c} \in \mathbb{R}_+^m \setminus \{\mathbf{0}\}$ such that $\mathbf{s} = \sum_i c_i \tilde{\mathbf{a}}_{(i)}$. Hence $\mathbf{v} \in \mathbb{S}_{\mathcal{J}}^{\perp} \setminus \{\mathbf{0}\}$ only if there exists $\mathbf{c} \in \mathbb{R}_+^m \setminus \{\mathbf{0}\}$ such that $\mathbf{s}^T \mathbf{v} = \sum_i c_i (\tilde{\mathbf{a}}_{(i)}^T \mathbf{v}) = 0$ which, as $\mathbf{c} \neq \mathbf{0}$, is only possible if $\exists i, k \in \mathbb{Z}_m$ such that $\text{sgn}(\tilde{\mathbf{a}}_{(i)}^T \mathbf{v}) \neq \text{sgn}(\tilde{\mathbf{a}}_{(k)}^T \mathbf{v})$. □

10 Experiments

10.1 Poloni's two objective function

The results of our algorithm on Poloni's two objective function [6]. Figure 8b shows more stable results for f_0 than f_1 . Likewise, in figure 8c stability of solutions in f_1 is favored over f_0 .

10.2 Progress of MOBO-PC

The calculation of hypervolume in MOBO-PC relies on both values of the weights for the Pareto front points and also the improved volume. That will result in favoring solutions complying with the constraints and assign them higher weights comparing to other Pareto front solutions. But if the

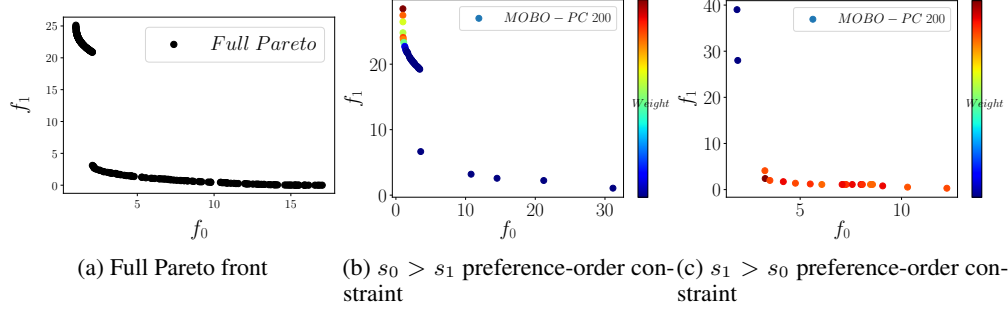


Figure 8: Obtained solutions for Poloni’s two objective function. 8a shows the full Pareto front. 8b illustrates the obtained solutions with $s_0 > s_1$ preference-order constraint on stability. And 8c shows the results of $s_1 > s_0$ or more stable solutions for f_1 .

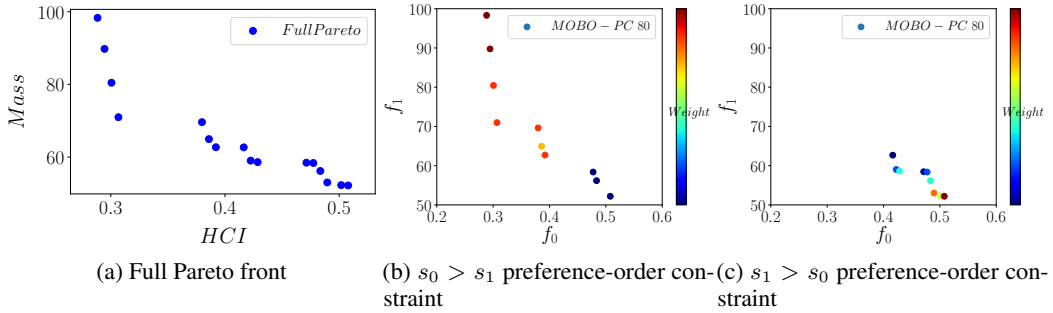


Figure 9: Obtained solutions for Simple Crash Study.

amount of volume to be improved is insignificant, the acquisition function favors solutions with lesser compliance with constraints but more possibility to increase the amount of volume -i.e. the region with most compliance with constraints is well explored and occupied with many Pareto front solutions, so the amount of hypervolume improvement drops due to the small amount of improvement in the volume despite of higher weights for the solutions in that region. Hence, the algorithm will then look for more diverse solutions that can increase the amount of hypervolume, that is the solutions which are more diverse and less stable. Figure 7 illustrates how acquisition function favors the points with higher weights at the first, and then lean towards the more unexplored regions with higher amount of hypervolume improvement.

11 Simple Crash Study

11.0.1 Summary

This problem concerns a collision in which a simplified vehicle moving at constant velocity crashes into a pole. The input parameters vary the strength of the bumper and hood of the car. During the crash, the front portion of the car deforms. The design goal is to maximise the *crashworthiness* of the vehicle. If the car is too rigid, the passenger experiences injury due to excessive forces during the impact. If the car is not rigid enough, the passenger may be crushed as the front of the car intrudes into the passenger space. This dataset is available in <https://bit.ly/2FWNXQS>.

11.0.2 Input Variables

- bumper is the mass of the front bumper bar. Range of bumper is between 1 and 5.
- thood is the mass of the front, hood and underside of the bonnet. Range of thood is between 1 and 5.

11.0.3 Output Responses

- Intrusion is the intrusion of the car frame into the passenger space. This is computed from the change in the separation of two points, one on the front of the car (Node #167) and one of the roof (Node #432). Lower intrusion is better. Increasing the mass of the hood and bumper will reduce the intrusion.
- HIC is the head injury coefficient. This is computed from the maximum deceleration during the collision. Lower HIC is better. Increasing the mass of the hood and bumper will increase the HIC.
- Mass is the combined mass of the front structural components. Lower mass is better.

In our experiment, we are using HIC as f_0 and Mass as f_1 to be minimised simultaneously.

Figure 9 shows the obtained results for this problem. Figure 9a illustrates full Pareto front, as 9b and 9c demonstrates our obtained results based on the defined preference-order constraints. Figure 9b shows that the Pareto front points are more stable in f_0 (HIC) than f_1 (Mass). As for figure 9c Pareto front solutions are in favor of stability for f_1 and more diversity for f_0 .